Research Article

Chemical Review and Letters
journal homepage: www.chemrevlett.com
ISSN (online): 2645-4947 (print) 2676-7279

Applying the $B_{12}N_{12}$ nanoparticle as the CO, CO_2, H_2O and NH_3 sensor

Rubabeh Rostamoghli[a], Mahshad Vakili[b], Alireza Banaei[a,] ∗, Eslam Pourbasheer [c], Khadadad Jalalierad [a]

[a] *Department of Science, Payame Noor University, P. O. Box: 19395-4697 Tehran, Iran*
[b] *Young Researchers and Elite club, Miyaneh Branch, Islamic Azad University, Miyaneh, Iran*
[c] *Department of Chemistry, Faculty of Science, University of Mohaghegh Ardabili, P.O. Box 179, Ardabil, Iran*

ARTICLE INFO

Article history:
Received 22 July
Received in revised form 30 August
Accepted 7 September
Available online 8 September

Keywords
carbon monoxide,
carbon dioxide,
water,
ammonia,
BNn,
M06-2X

ABSTRACT

In this study, the various properties including the stability energies, structural and electronic aspects of the hydrazine (N_2H_4), carbon monoxide (CO) water (H_2O) and ammonia (NH_3) molecules adsorptions on the top of the boron nitride nanoparticles (BNn) were studied through the Minnesota Functionals computations, DFT/M06-2X. The calculations clarifies that the most stable adsorption configurations are those in which the oxygen, carbon, oxygen and nitrogen atoms of CO_2, CO, H_2O and NH_3 are closed to the boron atom of the nanoparticle, respectively. The absorption energies were obtained about -0.14, -0.15, -0.87 and -1.54 eV for abosorption of CO_2, CO, H_2O and NH_3 gasses. The geometry optimizations, energy calculations and NBO charge transfer were used to evaluate the sensing ability of BNn for different analytes. The computed density of states (DOS) clarifies that a strong orbital hybridization take place between CO_2, CO, H_2O and NH_3 and BNn in adsorption process. Finally, it is concluded that the BNn nanoparticle has greater response selectivity toward NH_3 compared to CO, CO_2 and H_2O

1. Introduction

Boron is one of the very interesting elements in the periodic Table. Pure boron molecules are intermediate compounds between the materials with purely nonmetallic and metallic characteristics. This feature results into high chemical flexibility of boron rich molecules and it motives many researchers to search the ground-state geometries of boron rich molecules and reveal their unique characteristics [1-8].During the last decade, various experimental and theoretical efforts have been devoted to found the fullerene-like structures which formed of non-carbon elements [1–6]. In particular, the non-carbon elements in periodic table from III to V have been extensively applied in the fullerene-like cage and nanotube [7–13]. Especially, the group III nitrides have considerable importance to the science and technology aspects [14–16]. Boron nitride (BN) nanostructures such as nanotubes [17], nanocapsules [18] and electronic industry [19] have received much attention. The boron nitride nanostructures either nanocage or nanotubes are important due to their having temperature stability, high thermal conductivity and high resistance [17, 20–22]. The polar character of the B–N bonds in the boron nitride nanoparticles leads to a higher reactivity than their carbon homologues. In addition, the considerable charge difference between the nitrogen and boron atoms, the boron and nitrogen atoms can play as a Lewis acid and base role, respectively. Therefore, we can conclude that the boron nitride nanoparticles can be regarded as a non-metal catalyst. In the boron nitride category, $B_{12}N_{12}$ (BNn) was reported to be the smallest stable nanocage particles. Recently, the scrutiny of the poisionous gases is of the most importance in both industrial and living environments [24–27]. The presence of gases like carbon monoxide, carbon dioxide, nitrogen oxides and ammonia at any concentrations are damaging in the living environments. In the present research, we investigate the interactions between carbon monoxide (CO) carbon dioxide (CO_2), water (H_2O) and ammonia (NH_3) molecules and the BNn nanoparticle using M06-2X calculations. Evaluation of these gases is the basic function of the gas sensors [28]. The main purpose ofthis research is to obtain the fundamental outlooks into the efficacy of adsorbed gasses on the electronic

∗ Corresponding author. e-mail: banaei@pnu.ac.ir

aspects of the nanoparticles. The most valuable efforts are to use these effects to design more sensitive gas sensing devices.

2. Computational details

The theoretical calculations on the CO, CO_2, H_2O and NH_3 gasses and their complexes with BNn including CO_n–BNn or H_nX–BNn systems were carried out using a hybrid functional closed-shell M06-2X and 6-31++G** basis set, employing the Gaussian program pakage [16]. All the calculations were carried out in the gas phase under 1atm pressure and 298K temperature. The frequency calculations were performed at the mentioned level. No any pure imaginary frequency was obtained for the ground state at the same level of theory. Theoretical studies [17,18] proposed that the M06-2X method can give the best results to compute the absorption energies, strength of noncovalent interactions, and thermochemistry properties. The adsorption energies (E_{ad}) of the systems were computed using the M06-2X/6-31++G** level of theory. The E_{ad} was obtained via differences between the total energies of the CO_n–BNn or H_nX–BNn systems and the energies of each monomer. The interaction energies were corrected for the basis set superposition error (BSSE) in all the complexes using the full counterpoise method [19]. The density of states (DOS), molecular electrostatic potential surface (MEP) and frontier molecular orbital analyses were calculated and presented using the M06-2X/6-31+G* level of theory.

3. Results and discussion

3.1. Adsorptions in the COn–BNn (n = 1 and 2) or HnX–BNn (n = 2 and 3) systems

The fully optimized structure of isolated BNn nanoparticle is presented in Fig. 1a. The bond length of B–N shared between two six-membered rings is about 1.48 Å and that is shared between a four-membered ring and a six-membered rings is 1.43 Å. The calculated HOMO-LUMO gap energy (E_g) of pure BNn nanoparticle is to be about 9.15 eV, showing an insulator character. As shown in Fig. 3a, the HOMO and LUMO orbitals of pure BNn are localized on the N and B atoms, respectively. Thus, the electron deficient boron atoms can be regarded as a Lewis acid, whereas the electron-rich nitrogen atoms play the role of a Lewis base. These are consistent with the results obtained in Ahmadi et al. studies [36]. Because of the large difference in electronegativity between B and N, ionic bonding is predominant in the BNn nanoparticles. This can be seen from the surface electrostatic potentials (Fig. 2), where N sites receive electrons from B sites, resulting in positively charged B ions. These positively charged B ions on the cage surface become the available sites for adsorption of CO_2, CO, H_2O and NH_3 molecules. Also, the negativily charged N sites seem to be appropriate for adsorption H atoms of H_2O and NH_3 molecules. The interactions between the optimized structures of the BNn nanoparticles and CO_2, CO, H_2O and NH_3 is shown in Fig. 1 at the M062X/6-31+G* level of calculations. The calculated equilibrium molecule–cluster distance ($d_{Molecule/B_{12}N_{12}}$), adsorption energy ($E_{ad}$), NBO charge transfer, HOMO and LUMO energies, HOMO-LUMO gap energy (E_g) and change of E_g (ΔE_g) for each complex are presented in Table 1.

3.1.1. Adsorption of NH_3 on the nanoparticle

After the geometry optimization of the H_3N–BNn complex, two stable configurations were obtained for NH_3 from its N-side and H-side close to the B and N atoms of BNn nanoparticle, respectively which are presented in Figs. 1b and c. The adsorption energy and equilibrium distance of NH_3 from its N-side adsorption on the boron atom of BNn nanoparticles is -1.54 eV and 1.62 Å, respectively. The adsorption energy and equilibrium distance for H-side of NH_3 adsorption on the nitrogen atom of cage was -0.07 eV and 2.43 Å, respectively that can be defined as a hydrogen bond (Table 1). The boron atoms of nanoparticle acts as Lewis acid site and the nitrogen atom of NH_3 molecule acts as Lewis base site. In Fig. 2, we represented electrostatic potentials at the 0.001 electrons per $Bohr^{-3}$ isodensity surfaces of NH_3 adsorption on the BNn were calculated at the same level of theory with WFA surface analysis suite [37]. Natural bond orbital (NBO) analysis for N-side and H-side are 0.56 and -0.01 e, respectively. The results clarify that the hydrogen bond leads to decrease in the intensity of electrons at a particular position. For molecule adsorption on the sites of the cage surface can be explained by considering the fact that the highest occupied molecular orbitals (HOMOs) of the BNn are centered on the N sites, and the lowest unoccupied molecular orbitals (LUMOs) are located on the B sites (Fig. 3h). The NH_3 molecule can transfer the electrons to the LUMO on the N site of the cage through the electron lone pair of nitrogen atom and also hydrogen atom of NH_3 can accept electron from HOMO on the B site of the cage (Fig. 3j). The E_g for N-side and H-side of NH_3 are 7.72 and 5.91 eV, respectively (Table 1).

3.1.2. Adsorption of H_2O on the nanoparticle

The DFT calculations on the H_2O–BNn complex indicate that there are two adsorption sites between the oxygen and hydrogen atoms of H_2O (O-side and H-side) and the B and N atoms of BNn (Fig. 1d and 1e). In the H_2O adsorption systems, the bond lengths of B–O and N–H decrease by about 1.64 and 2.07 Å, respectively, that the adsorption energy (E_{ad}) are -0.87 and -0.18 eV, respectively (see Table 1). The NBO analysis shows that the oxygen and hydrogen atoms acquire positive and negative charges, respectively. This reveals that the charge is transferred from the H_2O molecule to the cage in the B–O bond formation while the in the N–H bond

formation the charge transferred from the cage to the H_2O molecule (Table 1). Fig. 2 presents the molecular electrostatic potentials V(r) on the surface of the BNn–H_2O, which are computed on the 0.001 au contour of the molecule's electronic density. The calculated HOMO-LUMO gap (E_g) for H_2O–BNn (O–B) and BNn–H_2O (N–H) systems are 7.88 and 9.19 eV. The results clarify that the E_g of H_2O–BNn (O–B) is significantly decreased through the adsorption process.

3.1.3. Adsorption of CO_2 on the nanoparticle

It is found two configurations through adsorption of CO_2 at top of the nanoparticle surface: (i) the carbon side (configuration d) and (ii) the oxygen side (configuration e) of CO_2 adsorption on the top of the boron atom of the nanoparticle (Fig. 1d and 1e). The M062X calculations indicate that the adsorption of the CO_2 molecule from the carbon side and oxygen side on the cages (d and e) are an exothermic processes with negative E_{ads} of -0.14 and -0.03 eV and the interaction distances are 2.54 and 4.19 Å, repectively (Fig. 1a). The NBO analysis indicates the charge transfers are 0.00 and 0.04 e from CO_2 to the BNn nanoparticles surfaces in the configurations d and e (Table 1). This charge transfer indicates that the boron atoms of nanoparticle acts as Lewis acid site and the carbon and oxygen atoms of CO_2 molecule acts as Lewis base site. Fig. 2 reveals the electrostatic potential map of the BNn-CO_2 system that indicates the locations of the various most positive and most negative potentials, designated as $V_{S,max}$ and $V_{S,min}$, respectively. The DFT calculations indicate that in the configuration e, the interaction between the molecule and cage is much stronger in comparison to that of the d configuration. The calculated HOMO of CO_2 molecule is mainly located on the oxygen atom; thus this reveals that the electrons are transferred from CO_2 molecule to the BNn nanoparticle (Figs. 3d and 3e).

3.1.4. Adsorption of CO on the nanoparticle

Two configurations were selected to investigate in adsorption of CO at top of the nanoparticle. In the configuration b, the carbon atom of CO attaches to the boron atom of the cage and in the configuration c, the oxygen atom of CO binds to the boron atom of the cage (Fig. 1b and c). The computed adsorption energies (E_{ad}) and the equilibrium molecule–cage distance ($d_{Molecule/B12N12}$) for the two molecular adsorption configurations are -0.15 eV and 1.81 Å for configuration b and -0.09 eV and 2.66 Å for configuration c (Table 1). The interaction between CO and BNn leads to a charge transfer of 1.20 and 0.02 from the carbon and oxygen sides of CO to the nanoparticle, respectively (Table 1). There is a positive electrostatic potential and negative electrostatic potential for this configuration (Fig. 2). The HOMO of CO molecule is mainly occurred on the carbon atom respect to oxgen atom which leads to the stronger interaction in configuration b in comparison to the configuration c. Comparative investigation of the adsorption energy in the COn–BNn (n = 1 and 2) or HnX–BNn (n = 2 and 3) systems reveals that BNn has greater response to NH_3 (from N side) than that of CO_2 (from C side), CO_2 (from O side), CO (from C side), CO (from O side) and H_2O (from O side) (Table 2). A relatively large difference of adsorption energy between COn–BNn or HnX–BNn complexes can be described based on the electronegativity difference, *p* character, and dipole moment in the molecules (see Table 2).

Table 1. Calculated adsorption energy (E_{ad}: eV), HOMO energies (E_{HOMO}), LUMO energies (E_{LUMO}) and HOMO–LUMO energy gap (E_g).

Comp.	E_{ad}	E_{HOMO} (eV)	E_{LUMO} (eV)	Eg (eV)	$\%\Delta E_g$ (eV)
BN	–	-9.51	-0.36	9.15	–
BN-NH_3	-1.54	-8.68	-0.95	7.72	142.59
BNn-H_3N	-0.07	-7.19	-1.28	5.91	324.18
BNn-OH_2	-0.87	-8.86	-0.99	7.88	127.05
BNn-H_2O	-0.15	-8.11	-1.41	6.70	245.29
BNn-CO_2	-0.03	-9.53	-0.47	9.06	8.68
BNn-O_2C	-0.14	-9.44	-0.44	9.00	14.69
BNn-CO	-0.15	-9.14	-0.05	9.09	5.87
BNn-OC	-0.09	-9.45	-0.01	9.44	29.01

3.2. Density of state (DOS) analysis

Computed density of state (DOS) maps indicate that the energy gaps of BNn is 9.15 eV and of COn–BNn or HnX–BNn with CO_2 (C–side interaction), CO_2(O–side interaction), CO(C–side interaction), CO(O–side interaction), NH_3(N–side interaction), H_2O (O–side interaction) NH_3 (H–side interaction) and H_2O (H–side interaction) complexes are 9.15, 9.06, 9.00, 9.09, 9.44,7.88, 7.72, 5.91 and 6.70 eV, respectively at the M06-2X/6-31++G** method (Fig. 3).

The ΔE_g in the adsorption process is associated to the sensitivity of an absorbent for a particular molecule. As seen in Table 1, the ΔE_g of BNn is 8.68% and of COn–BNn or HnX–BNn with CO_2 (C–side interaction), CO_2(O–side interaction), CO(C–side interaction), CO(O–side interaction), NH_3(N–side interaction), H_2O (O–side interaction) NH_3 (H–side interaction) and H_2O (H–side interaction) complexes are 14.69%, 5.87%, 29.01%, 127.05%, 142.59% 324.18% and 245.29%, respectively. The computed DOS indicates that the E_g amount is reduced compared to the isolated BNn. It is known that the E_g is a major factor in determiniation of the electrical conductivity of BNn which will improve in the existance of the molecules with respect to the following equation [38]:

$$\sigma \propto \exp\left(\frac{-E_g}{2KT}\right)$$

in where σ is the electrical conductivity and k is the Boltzmann's constant. According to the equation, the smaller E_g amount leads to increase the conductivity at a given temperature. However, it can be conclude that the BNn nanoparticle selectively acts as a gas sensor device between CO_2, CO, H_2O and NH_3 which acts as the most suitable gas sensor for the NH_3 molecule.

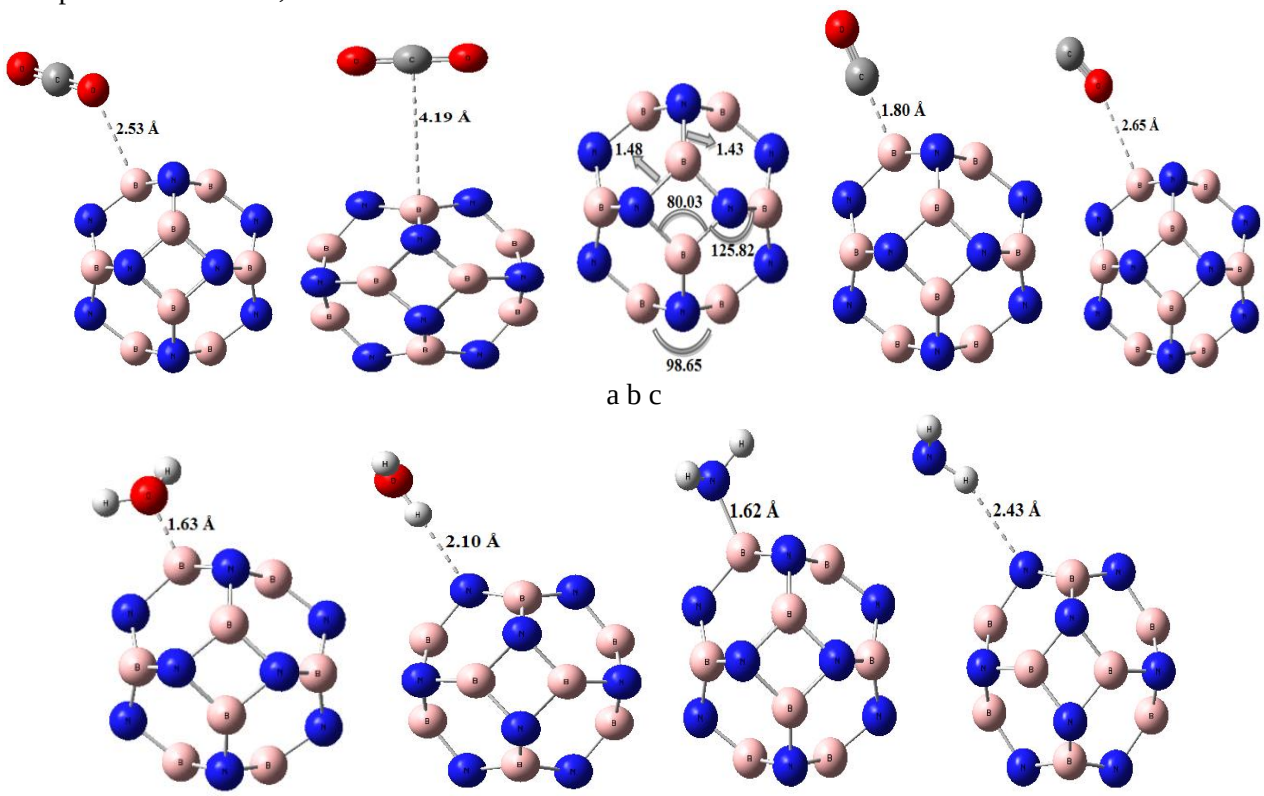

Fig. 1. Geometric parameters of isolated BNn and small molecule-adsorbed BNn nanoparticle. Distances in Å and angles in degrees.

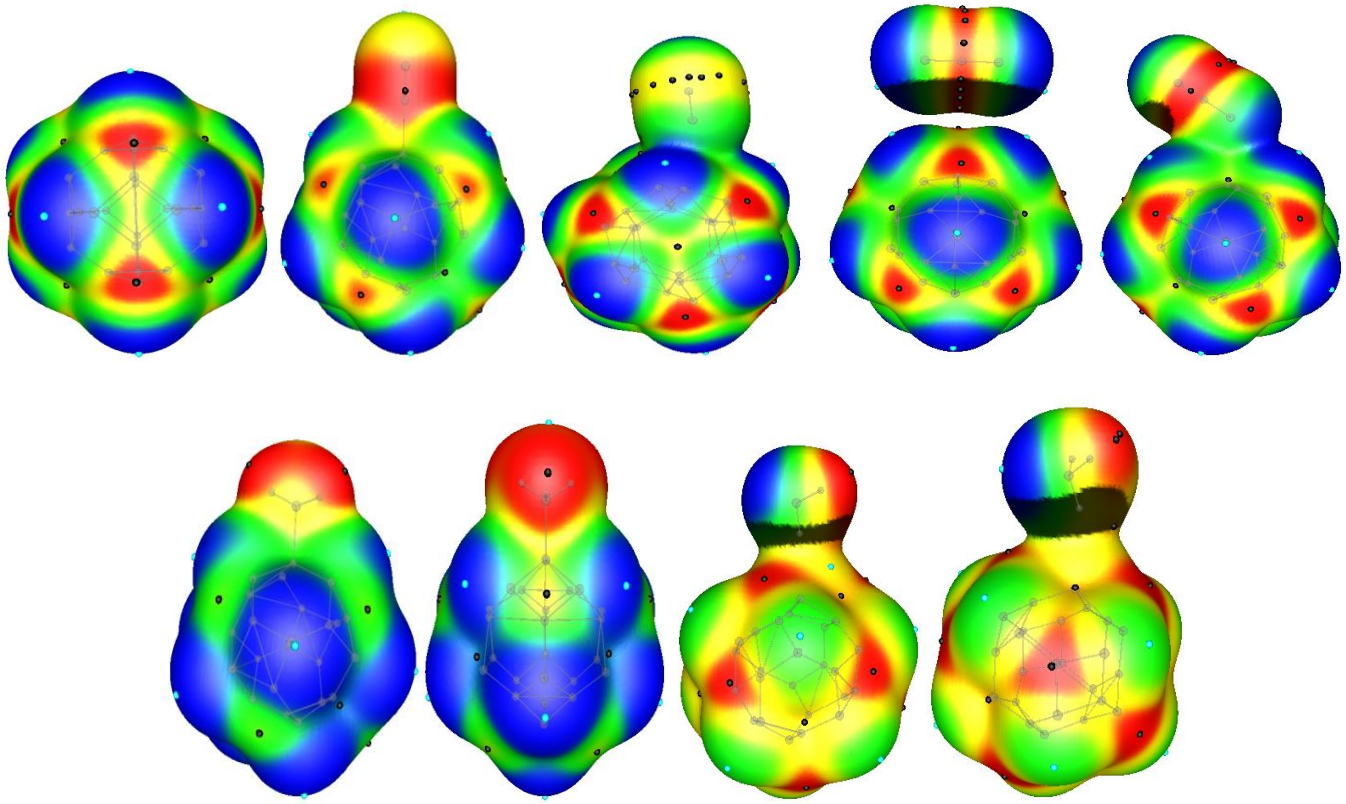

Fig. 2. The molecular electrostatic potentials V(r) on the surface of the BNn-Complexes.

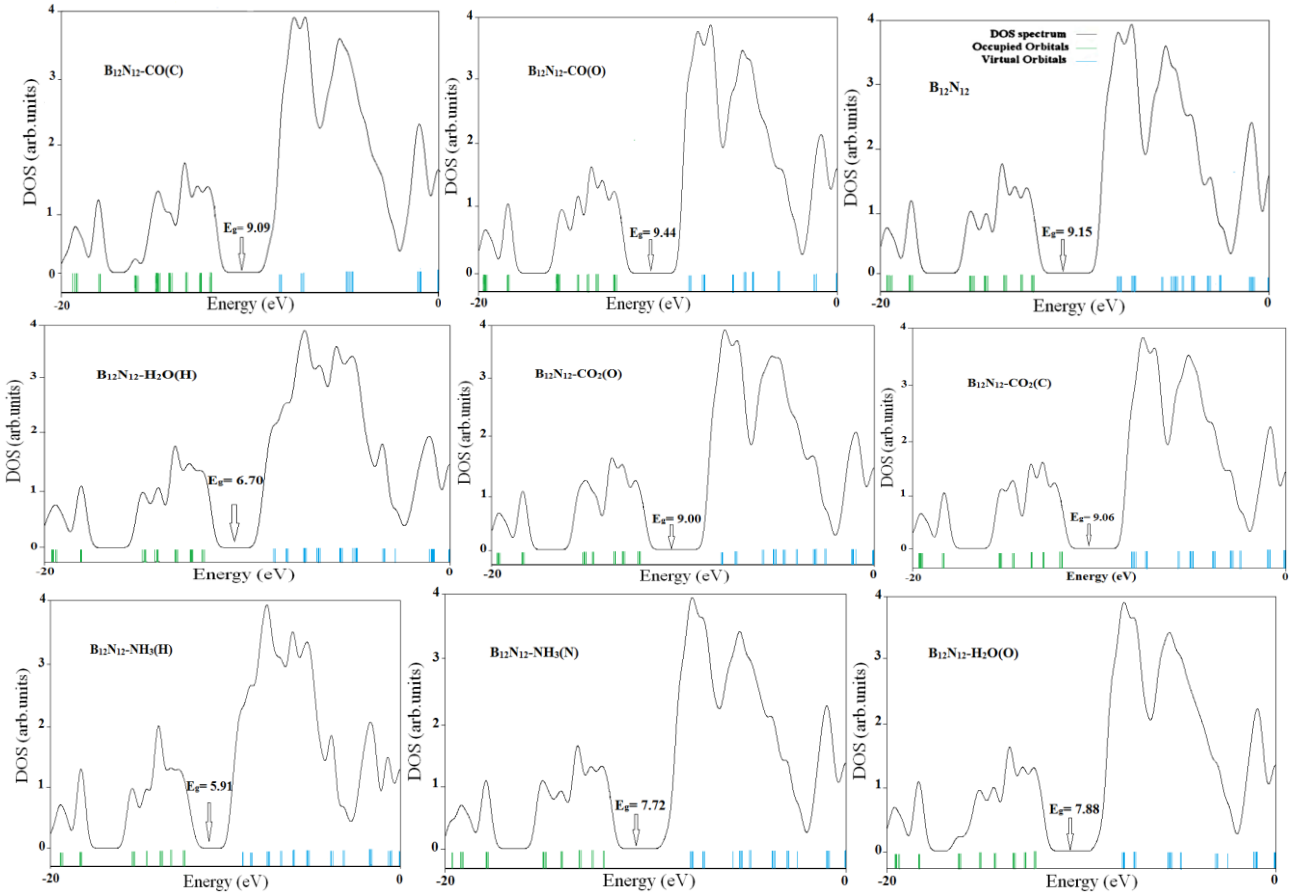

Fig. 3. Computed density of states (DOS) for pure BNN and the BNN- CO(C), BNN-CO(O), BNN-CO_2(C), BNN-CO_2(O), BNN-NH_3(N), BNN- H_2O(O), BNN-NH_3(H) and BNN-H_2O(H) complexes

4. Conclusions

The M06-2X calculations are used to studied the equilibrium distances, stabilities, and electronic properties of CO_2, CO, NH_3 and H_2O molecules which adsorbed at top of the BNn nanoparticle. The results reveal that the CO_2, CO, NH_3 and H_2O molecules can be strongly adsorbed on the BNn with a good adsorption energies. The CO and CO_2 molecules interactions to BNn from the carbon and oxygen atoms of CO and CO_2 are more prominent compared to the interaction with the oxygen and carbon atoms, respectively. A relatively large difference of adsorption energy between COn–BNn (n = 1 and 2) or HnX–BNn (n = 2 and 3) complexes can be described on the basis of electronegativity difference, p character, and dipole moment in molecules. The most stable configuration was BNn-NH_3 with E_{ad} and E_g about -1.54 and 7.72 eV and 142.59% change of the E_g. Finally, it is concluded that BNn nanoparticle has greater response selectivity toward NH_3 compared to CO, CO_2 and H_2O , a wide variety of investigations have been done upon the adsorption of this molecule both theoretically and experimentally.

References

[1] I. Torkpoor, M. Heidari Nezhad Janjanpour, N. Salehi, F. Gharibzadeh, L. Edjlali, Insight into Y@X2B8 (Y= Li, CO2 and Li-CO2, X = Be, B and C) nanostructures: A computational study. *Chem. Rev. Lett.*, 1 (2018) 2-8.

[2] F. Gharibzadeh, S. Gohari, K. Nejati, B. Hashemzadeh, S. Mohammadiyan, The Be atom doping: An effective way to improve the Li-atom adsorption in boron rich nanoflake of B24. *Chem. Rev. Lett.*, 1 (2018) 16-22.

[3] S. HaiJun, Thermal-conductivity and tensile-properties of BN, SiC and Ge nanotubes. Comp. *Mater. Sci.*, 47 (2009) 220–224.

[4] D. Golberg, Y. Bando, Octahedral boron nitride fullerenes formed by electron beam irradiation. *Appl. Phys. Lett.* 73 (1998) 2441–2443.

[5] H. Omidvar, S. Goodarzi, A. Seif, A.R. Azadmehr, Influence of anodization parameters on the morphology of TiO2 nanotube arrays. *Superlattice. Microst.* 50 (2011) 26–39.

[6] S.K. Jain, P. Srivastava Electronic and optical properties of ultrathin single walled boron nanotubes – An ab initio study. *Comp. Mater. Sci.* 50 (2011) 3038–3042.

[7] J. Beheshtian, Z. Bagheri, M. Kamfiroozi, A. Ahmadi, *J. Mol. Model.* 18 (2012) 2653-2658.

[8] G. Seifert, E. Hernandez, Theoretical prediction of phosphorus nanotubes. *Chem. Phys. Lett.* 318 (2000) 355–360.

[9] H.S. Wu, F.Q. Zhang, X.H. Xu, C.J. Zhang, H. Jiao, Geometric and Energetic Aspects of Aluminum Nitride Cages. *J. Phys. Chem. A.*, 107 (2003) 204–209.

[10] Y.R. Hacohen, E. Grunbaum, R. Tenne, J.L. Hutchison, Cage structures and nanotubes of NiCl2, *Nature.*, 395 (1998) 336–337.
[11] Y. Feldman, E. Wasserman, D.J. Srolovitz, R. Tenne, High-rate, gas-phase growth of MoS2 nested inorganic fullerenes and nanotubes. *Science.*, 267 (1995) 222–225.
[12] C. Balasubramanian, S. Belluci, P. Castrucci, M.D. Crescenzi, S.V. Bhoraskar, *Chem. Phys. Lett.* 383 (2004) 188–191.
[13] L. Bourgeois, Y. Bando, W.Q. Han, T. Sato, Structure of boron nitride nanoscale cones: Ordered stacking of 240° and 300° Disclinations. *Phys. Rev., B* 61 (2000) 7686–7691.
[14] D.A. Neumayer, J.G. Ekerdt, Growth of Group III Nitrides. A Review of Precursors and Techniques. *Chem. Mater.*, 8 (1996) 9–25.
[15] W.H. Goh, G. Patriarche, P.L. Bonanno, S. Gautier, T. Moudakir, M. Abid, G. Orsal, A.A. Sirenko, Z.H. Cai, A. Martinez, A. Ramdane, L. Le Gratiet, D. Troadec, A. Soltani, A. Ougazzaden, Structural and optical properties of nanodots, nanowires, and multi-quantum wells of III-nitride grown by MOVPE nano-selective area growth. *J. Cryst., Growth* 315 (2011) 160–163.
[16] E. Silva Pinto, R. de Paiva, L.C. de Carvalho, H.W.L. Alves, J.L.A. Alves, Theoretical optical parameters for III-nitride semiconductors. *Microelectr. J.* 34 (2003) 721–724.
[17] N. G.Chopra, R. J. Luyken, K. Cherrey, V. H. Crespi, M.L. Cohen, S.G. Louie, A. Zettl, Boron Nitride Nanotubes. *Science.*, 269 (1995) 966.
[18] I. Narita, T. Oku, Effects of catalytic metals for synthesis of BN fullerene nanomaterials. *Diamond. Relat. Mater.*, 12 (2003) 1146.
[19] S. Iijima, C. J. Brabec, A.Maiti, J. Bernholc, Structural flexibility of carbon nanotubes. *J. Chem. Phys.*, 104 (1996) 2089.
[20] D. Golberg, Y. Bando, O. Stephan, K. Kurashima, Octahedral boron nitride fullerenes formed by electron beam irradiation. *Appl. Phys. Lett.*, 73 (1998) 2441.
[21] D. Golberg, Y. Bando, K. Kurashima, T. Sato, Synthesis and characterization of ropes made of BN multiwalled nanotubes. *Scr. Mater*., 44 (2001) 1561.
[22] D. B. Zhang, E. Akatyeva, T. Dumitrica, Surface physics, nanoscale physics, low-dimensional systems-Routes to identification of intrinsic twist in helical MoS2 nanotubes by electron diffraction and annular dark-field scanning transmission electron microscopy imaging. *Phys, Rev.*, B 84 (2011) 115431.
[23] T. Oku, A. Nishiwaki, I. Narita, M. Gonda, Formation and structure of B24N24 clusters. *Chem. Phys. Lett.* 380 (2003) 620-623.
[24] M. Neek-Amal, J. Beheshtian, A. Sadeghi, K. Michel, F.M. Peeters, Boron Nitride Monolayer: A Strain-Tunable Nanosensor. *J. Phys. Chem. C.*, 117 (2013) 13261–13267.
[25] D. Kohl, TOPICAL REVIEW: Function and applications of gas sensors. *J. Phys.*, D34 (2001) R125–R149.
[26] A. Dubbe, Fundamentals of solid state ionic micro gas sensors. *Sens. Actuat. B.*, 88 (2003) 138 –148.
[27] Q. Wan, Q.H. Li, Y.J. Chen, T.H. Wang, X.L. He, J.P. Li, C.L. Lin, Miniaturized gas ionization sensors using carbon nanotubes. *Nature.*, 424 (2003) 171–174.
[28] H. Ullah, K. Ayub, Z. Ullah, M. Hanif, R. Nawaz, A.A. Shah, S. Bilal, Theoretical insight of polypyrrole ammonia gas sensor. *Synth. Met.* 172 (2013) 14–20.
[29] M.J. Frisch, G.W. Trucks, H.B. Schlegel, G.E. Scuseria, M.A. Robb, J.R. Cheeseman, G. Scalmani, V. Barone, B. Mennucci, G.A. Petersson, H. Nakatsuji, M. Caricato, X. Li, H.P. Hratchian, A.F. Izmaylov, J. Bloino, G. Zheng, J.L. Sonnenberg, M. Hada, M. Ehara, K. Toyota, R. Fukuda, J. Hasegawa, M. Ishida, T. Nakajima, Y. Honda, O. Kitao, H. Nakai, T. Vreven, J.A. Montgomery Jr., J.E. Peralta, F. Ogliaro, M. Bearpark, J.J. Heyd, E. Brothers, K.N. Kudin, V.N. Staroverov, R. Kobayashi, J. Normand, K. Raghavachari, A. Rendell, J.C. Burant, S.S. Iyengar, J. Tomasi, M. Cossi, N. Rega, J.M. Millam, M. Klene, J.E. Knox, J.B. Cross, V. Bakken, C. Adamo, J. Jaramillo, R. Gomperts, R.E. Stratmann, O. Yazyev, A. J. Austin, R. Cammi, C. Pomelli, J.W. Ochterski, R.L. Martin, K. Morokuma, V. G. Zakrzewski, G.A. Voth, P. Salvador, J.J. Dannenberg, S. Dapprich, A.D. Daniels, Ö. Farkas, J.B. Foresman, J.V. Ortiz, J. Cioslowski, D.J. Fox, Gaussian, Gaussian Inc., Wallingford, CT, (2009).
[30] S. Kozuch, J.M.L. Martin, Halogen bonds: Benchmarks and theoretical analysis. *J. Chem. Theor. Comput.* 9 (2013) 1918-1931.
[31] M.D. Esrafili, R. Nurazar, Potential of C-doped boron nitride fullerene as a catalyst for methanol dehydrogenation. *Comput. Mater. Sci.* 92 (2014) 172-177.
[32] M.W. Schmidt, K.K. Baldridge, J.A. Boatz, S.T. Elbert, M.S. Gordon, J.H. Jensen, S. Koseki, N. Matsunaga, K.A. Nguyen, S.J. Su, T.L. Windus, M. Dupuis, J.A. Montgomery, General atomic and molecular electronic structure system. *J. Comput. Chem.*, 14 (1993) 1347–1363.
[33] F. Weinhold, C.R. Landis, Discovering Chemistry With Natural Bond Orbitals, John Wiley & Sons, (2012).
[34] Z. Jin, Y. Su, Y. Duan, Development of a polyaniline-based optical ammonia sensor. *Sens. Actuat. B.*, 72 (2001) 75–79.
[35] N. O'Boyle, A. Tenderholt and K. Langner, cclib: A library for package independent computational chemistry algorithms. *J. Comput. Chem.* 29 (2008) 839–845.
[36] Javad Beheshtian, Zargham Bagheri, Mohammad Kamfiroozi, Ali Ahmadi, Toxic CO detection by B12N12 nanocluster. *Microelectr. J.*, 42 (2011) 1400–1403.
[37] Bulat FA, Toro-Labbe A, Brinck T, Murray JS, Politzer P Quantitative analysis of molecular surfaces: areas, volumes, electrostatic potentials and average local ionization energies. *J. Mol. Model.* 16 (2010) 1679–1691.
[38] S.S. Li, Semiconductor physical electronics, 2nd edn. Springer, Heidelberg (2006).

How to Cite This Article

Robabeh Rostamoghli; Mahshad Vakili; Alireza Banaei; Eslam Pourbashir; Khodadad Jalalierad. "Applying the B12N12 nanoparticle as the CO, CO2, H2O and NH3 sensor". Chemical Review and Letters, 1, 1, 2018, 31-36. doi: 10.22034/crl.2018.85214